Disease Models & Mechanisms 4, 526-536 (2011) doi:10.1242/dmm.006676

Zebrafish embryo screen for mycobacterial genes involved in the initiation of granuloma formation reveals a newly identified ESX-1 component

Esther J. M. Stoop[1], Tim Schipper[1], Sietske K. Rosendahl Huber[1], Alexander E. Nezhinsky[2], Fons J. Verbeek[2], Sudagar S. Gurcha[3], Gurdyal S. Besra[3], Christina M. J. E. Vandenbroucke-Grauls[1], Wilbert Bitter[1] and Astrid M. van der Sar[1,*]

SUMMARY

The hallmark of tuberculosis (TB) is the formation of granulomas, which are clusters of infected macrophages surrounded by additional macrophages, neutrophils and lymphocytes. Although it has long been thought that granulomas are beneficial for the host, there is evidence that mycobacteria also promote the formation of these structures. In this study, we aimed to identify new mycobacterial factors involved in the initial stages of granuloma formation. We exploited the zebrafish embryo *Mycobacterium marinum* infection model to study initiation of granuloma formation and developed an in vivo screen to select for random *M. marinum* mutants that were unable to induce granuloma formation efficiently. Upon screening 200 mutants, three mutants repeatedly initiated reduced granuloma formation. One of the mutants was found to be defective in the *espL* gene, which is located in the ESX-1 cluster. The ESX-1 cluster is disrupted in the *Mycobacterium bovis* BCG vaccine strain and encodes a specialized secretion system known to be important for granuloma formation and virulence. Although *espL* has not been implicated in protein secretion before, we observed a strong effect on the secretion of the ESX-1 substrates ESAT-6 and EspE. We conclude that our zebrafish embryo *M. marinum* screen is a useful tool to identify mycobacterial genes involved in the initial stages of granuloma formation and that we have identified a new component of the ESX-1 secretion system. We are confident that our approach will contribute to the knowledge of mycobacterial virulence and could be helpful for the development of new TB vaccines.

INTRODUCTION

Mycobacterium tuberculosis is the causative agent of tuberculosis (TB) and is responsible for about 1.6 million deaths annually (WHO: http://www.who.int/tb/publications). Therefore, TB remains a major global health problem and, despite renewed interest in this ancient disease, we do not fully understand the exact mechanism of mycobacterial virulence. Upon infection via inhalation of droplets containing *M. tuberculosis*, bacteria are taken up by patrolling alveolar macrophages. Even though the alveolar macrophages are dedicated phagocytic cells with a range of antibacterial weapons, pathogenic mycobacteria are able to persist and replicate in these cells. The infected macrophages become activated and subsequently recruit additional macrophages, neutrophils and lymphocytes. Together, these cells form well organized, tight aggregates called granulomas. These granulomas are the hallmark of tuberculosis (Adams, 1976).

Because granuloma formation seems to be orchestrated by the immune system, they have long been considered to be host beneficial, and able to control bacterial replication and dissemination (Saunders et al., 1999). However, various recent studies imply that granuloma formation is also important for bacterial survival and person-to-person spread. Bacteria inside granulomas are able to prevent eradication by the immune system and, moreover, aggregation of macrophages is in fact crucial for mycobacterial dissemination (Volkman et al., 2004; Flynn and Chan, 2005; Kahnert et al., 2007; Davis and Ramakrishnan, 2009). In line with this view, bacterial virulence factors have been identified that promote the formation of granulomas (Volkman et al., 2004; Swaim et al., 2006).

The most well studied genetic locus involved in mycobacterial virulence and granuloma formation is probably region of difference 1 (RD1). This region, which spans nine genes, is deleted in all attenuated *Mycobacterium bovis* bacille Calmette-Guérin (BCG) vaccine strains (Mahairas et al., 1996). Reintroduction of an intact version of RD1 into *M. bovis* BCG resulted in increased bacterial growth and formation of granuloma-like structures in immunodeficient mice (Pym et al., 2002), whereas deletion of RD1 from *M. tuberculosis* led to attenuation of both bacterial replication and granuloma formation in a mouse infection model (Lewis et al., 2003). Also *Mycobacterium marinum*, the causative agent of fish tuberculosis, shows delayed granuloma formation in zebrafish (*Danio rerio*) when RD1 is absent (Gao et al., 2004; Volkman et al., 2004; Swaim et al., 2006). The nine genes of the RD1 region are part of the ESX-1 locus, which encodes a specialized secretion system responsible for the secretion of a number of proteins, including the important virulence factors ESAT-6 and CFP-10.

[1]Department of Medical Microbiology and Infection Control, VU University Medical Center, van der Boechorststraat 7, 1081 BT Amsterdam, The Netherlands
[2]Section Imaging and Bioinformatics, Leiden Institute for Advanced Computer Science, Leiden University, Niels Bohrweg 1, 2333 CA Leiden, The Netherlands
[3]School of Biosciences, University of Birmingham, Edgbaston, Birmingham, B15 2TT, UK
*Author for correspondence (a.vandersar@vumc.nl)

Received 30 August 2010; Accepted 1 February 2011

These two secreted proteins are encoded by genes of the RD1 region. It has been reported that ESAT-6 is involved in the disruption of membranes; consequently, the protein has been associated with the translocation of mycobacteria from the phagosome into the cytosol and subsequent intercellular spread (Hsu et al., 2003; Gao et al., 2004; van der Wel et al., 2007; Smith et al., 2008). These effector functions might explain the mechanism of virulence of ESX-1.

Although ESX-1 is an important virulence factor of mycobacteria, other factors will also be involved in virulence. Our aim is to identify new mycobacterial virulence determinants, and in particular bacterial factors involved in granuloma formation. Because establishment of granulomas involves a complex interaction between host and microbe, this objective requires an in vivo approach.

In the past years, the *M. marinum* zebrafish model has been established as a useful model for the study of mycobacterial infections. *M. marinum* is a close genetic relative of *M. tuberculosis* and, in ectotherms, causes a tuberculosis-like disease characterized by granuloma formation (Ramakrishnan et al., 1997; Talaat et al., 1998; Davis et al., 2002; Prouty et al., 2003; van der Sar et al., 2004; Broussard and Ennis, 2007). The zebrafish is one of the natural hosts of *M. marinum*, in which the pathogen produces caseating granulomas that resemble human granulomas (Davis et al., 2002; Prouty et al., 2003; van der Sar et al., 2004; Swaim et al., 2006). One of the advantages of working with zebrafish is that their embryos have not yet developed an adaptive immune system (Trede et al., 2004), which enables the investigation of the role of the innate immune response during mycobacterial disease separately from the role of the adaptive system. Additionally, zebrafish embryos are transparent, which makes it possible to follow early stages of *M. marinum* infection in real-time. These early infection stages include the formation of aggregates of infected macrophages. Interestingly, it has been reported that *M. marinum* that is phagocytosed by macrophages and is present within these aggregates induces the upregulation of genes that were found to be specifically expressed in mature granulomas (Davis et al., 2002). Therefore, the zebrafish *M. marinum* model is an excellent model for studying mycobacterial pathogenesis.

In this study, we have set up a screen to identify mycobacterial genes involved in the onset of granuloma formation. We screened a transposon mutant library of *M. marinum* in zebrafish embryos for mutants with impaired initiation of granuloma formation. Upon screening 200 mutants, we identified three mutants that repeatedly induced less granuloma formation. In one of these mutants a mutation in the ESX-1 region was found to be responsible for the observed phenotype and ESAT-6 secretion was severely affected in this mutant.

RESULTS

Screen for *M. marinum* mutants attenuated for granuloma formation in zebrafish embryos

In order to detect mycobacterial factors involved in granuloma formation, we used the well described zebrafish embryo *M. marinum* infection model. Zebrafish embryos were injected into the caudal vein (Fig. 1A) immediately after the onset of blood circulation, i.e. at 28 hours post fertilization (hpf), with different isolates of *M. marinum* expressing DsRed. To optimize the infection model for granuloma formation, seven different *M. marinum* strains were analyzed for their potential to initiate granulomas in embryos. These strains were similar to those used in a previous study involving adult zebrafish (van der Sar et al., 2004). Clustering of macrophages infected with mycobacteria was used as an indicator of initial granuloma formation, and was examined by fluorescence microscopy at 5 days post infection (dpi). Although all strains showed bacterial clustering, there was considerable variability in the amount of initial granuloma formation (data not shown). For further experiments, we selected strain E11 because this isolate caused highly reproducible clustering of bacteria, at inocula ranging from 50 to 200 colony forming units (CFUs) (Fig. 1B). Moreover, *M. marinum* strain E11 (also known as Mma11) induces chronic infection with necrotizing granulomas in adult zebrafish (van der Sar et al., 2004), which is also the case for granulomas found in human TB patients.

To verify our granuloma model, it was important to determine whether the aggregation of mycobacteria that we observed by fluorescence microscopy actually represents early granuloma formation. Therefore, we monitored the activity of an *M. marinum* granuloma-activated promoter (*gap*) with a *gap-eGFP* construct as was described previously (Ramakrishnan et al., 2000; Chan et al., 2002; Davis et al., 2002). Because the *gap* promoter is specifically active in granulomas and not in macrophages or in in vitro conditions, expression of eGFP in aggregated mycobacteria indicates granuloma-like conditions. Zebrafish embryos were infected with Mma11 modified to constitutively express DsRed and express eGFP under the control of *gap7*. At day 5 of infection we observed that, in the clusters of red fluorescent mycobacteria, the majority of the bacteria expressed eGFP (Fig. 1C). This demonstrates that these mycobacteria encounter conditions that are similar to those in mature granulomas.

Furthermore, to ensure the usability of this model for the identification of early granuloma mutants, we investigated the ability of a negative control to initiate granuloma formation. For this experiment, we infected zebrafish embryos with an Mma11 mutant that has a mariner transposon insertion in gene *eccCb1* (A.M.v.d.S., unpublished), one of the essential components of the ESX-1 system (Stanley et al., 2003). As shown in Fig. 1D, bacterial clustering was drastically reduced in the *eccCb1*::tn mutant at 5 dpi, which indicates that our embryo model can indeed be used to identify mutants in initial granuloma formation. The reduced bacterial clustering of the *eccCb1*::tn mutant is consistent with a previous study in which infection of zebrafish embryos with an ESX-1 mutant in the *M. marinum* M strain resulted in reduced formation of early granulomas (Volkman et al., 2004).

In order to analyze bacterial infection in a quantitative and objective manner, two complementary methods were used. First, fluorescent images of infected embryos were subjected to automated analysis with software that was exclusively designed for this purpose. Second, the amount of bacteria within infected embryos was measured by plating whole embryos and counting CFUs. According to the software program, the *eccCb1*::tn mutant induces only 3.5% of the infection rate of wild-type bacteria (Fig. 1E). This number is highly comparable to the ratio of bacterial loads of infected embryos as determined by plating (95.3 CFUs per embryo for the *eccCb1*::tn mutant versus 1718 CFUs per embryo for the wild type, which represents 5.5%; see Fig. 1F). Consequently,

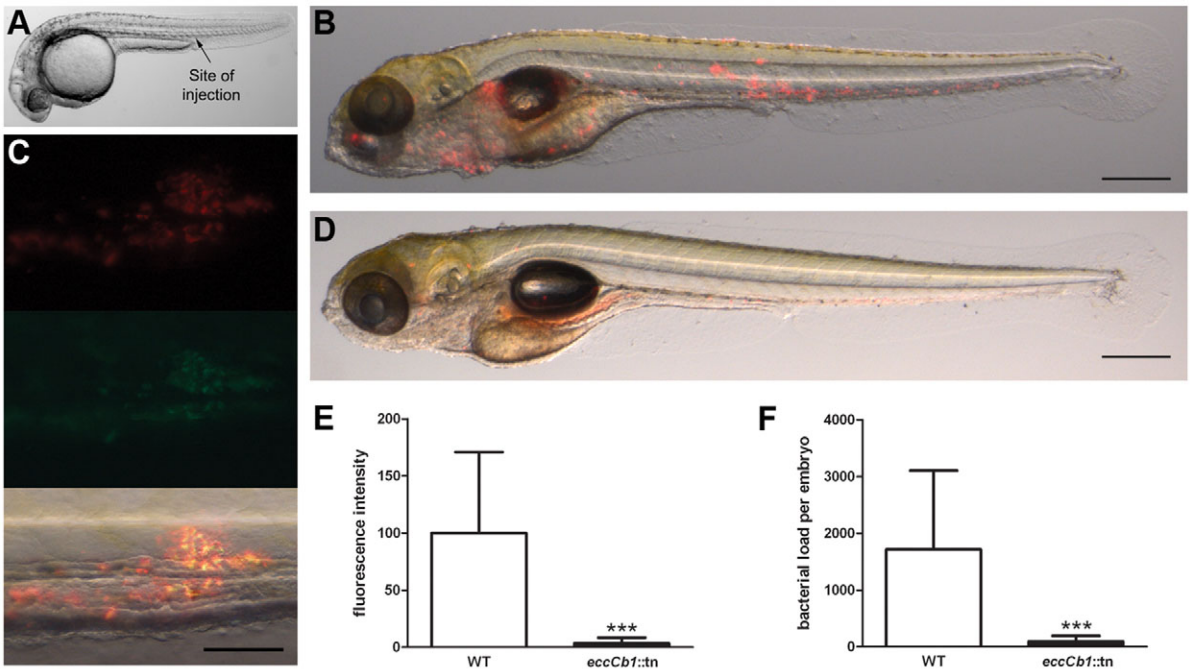

Fig. 1. Initiation of granuloma formation in *M. marinum* E11 (Mma11)-infected embryos. (A) Overview of a zebrafish embryo at 28 hpf. The arrow indicates the caudal vein injection site used in this study. (B) Embryo 5 days after infection with 110 CFUs Mma11. Overlay of brightfield and fluorescent images is shown. Aggregates of red fluorescent bacteria are seen in the tail and head region. Scale bar: 500 µm. (C) Bacterial clustering in tail at 5 dpi with 92 CFUs Mma11 expressing hsp::DsRed and gap7::eGFP. Of the total amount of bacteria [constitutively expressing red fluorescence (top panel)], the majority expresses eGFP (middle panel), indicating that the bacteria reside in clusters that resemble granulomas. Overlay shows overlapping red and green fluorescence as yellow (bottom panel). Scale bar: 50 µm. (D) The Mma11 *eccCb1*::tn mutant is highly attenuated for initiation of granuloma formation at 5 dpi with 171 CFUs. Loose spots of red fluorescent bacteria are detected, but aggregates are not found. Scale bar: 500 µm. (E) Quantification of infection as determined with specially designed software. The amount of red (fluorescent) pixels of fluorescent images of embryos infected with the *eccCb1*::tn mutant is set as a percentage of the amount of red pixels of fluorescent images of embryos infected with wild-type bacteria (WT). Data shown are mean + standard deviation of three independent experiments (***P<0.001, unpaired Student's *t*-test). (F) From embryos used in E, bacterial loads were determined by plating whole embryos (***P<0.001, unpaired Student's *t*-test).

this automated analysis enables us to screen numerous mutants simultaneously and to rapidly select for early-granuloma-deficient mutants without any bias.

Having set up an early granuloma model, we screened a mariner transposon library of Mma11 modified to constitutively express DsRed. We performed mono-infections because co-infection with multiple mutants can obscure the granuloma phenotype, owing to the wild-type helper effect. Per mutant, a group of 15 embryos was infected with approximately 100 CFUs and early granuloma mutants were rescreened at least twice. Screening of the first 200 mutants resulted in the identification of three early granuloma mutants, named FAM53, FAM58 and FAM67, that repeatedly showed a reduced ability to induce granuloma formation (Fig. 2A-C). The infection levels of embryos infected with the mutant strains were 20-46% of the parental Mma11 infection level (Fig. 2D).

Early granuloma mutants are not essentially defective for intracellular growth or spread

The aim of this screen was to identify mutants that are specifically attenuated for granuloma formation in vivo. However, it would also probably identify mutants deficient in survival in macrophages or dissemination to uninfected macrophages. In order to differentiate between these two classes of mutants, we performed in vitro infection experiments. Because macrophages are the primary cells for intracellular growth of mycobacteria during disease, we used the human monocytic cell line THP1 in our in vitro experiments. Activated THP1 cells were infected for 2 hours with the different early granuloma mutants at a multiplicity of infection (MOI) of 1. At 0, 24, 48 and 72 hours post infection (hpi), intracellular growth and spread of the bacteria were examined.

CFU counting of THP1 cell lysates indicated that none of the early granuloma mutants has a severe replication defect in host cells (Fig. 3A). Only mutant FAM58 displayed a moderate decrease in growth. By contrast, intracellular replication of the Mma11 *eccCb1*::tn mutant was drastically reduced as compared with that of the wild-type strain (Fig. 3A). This variation in intracellular growth was specific for infected cells, because all mutants demonstrated broadly comparable growth rates in liquid culture (Fig. 3B).

In order to assay intercellular spread of the mutants, the percentage of infected THP1 cells was examined by fluorescence microscopy. At 48 hpi, the percentage of THP1 cells infected with wild-type *M. marinum* reached approximately 100% (Fig. 3C). Consistent with the CFU experiments, FAM53 and FAM67 disseminated equally well. In marked contrast to the parental Mma11 strain, intercellular spread of the *eccCb1*::tn mutant was strongly attenuated. In THP1 cells infected with mutant FAM58, an intermediate level of bacterial dissemination was observed (Fig. 3C).

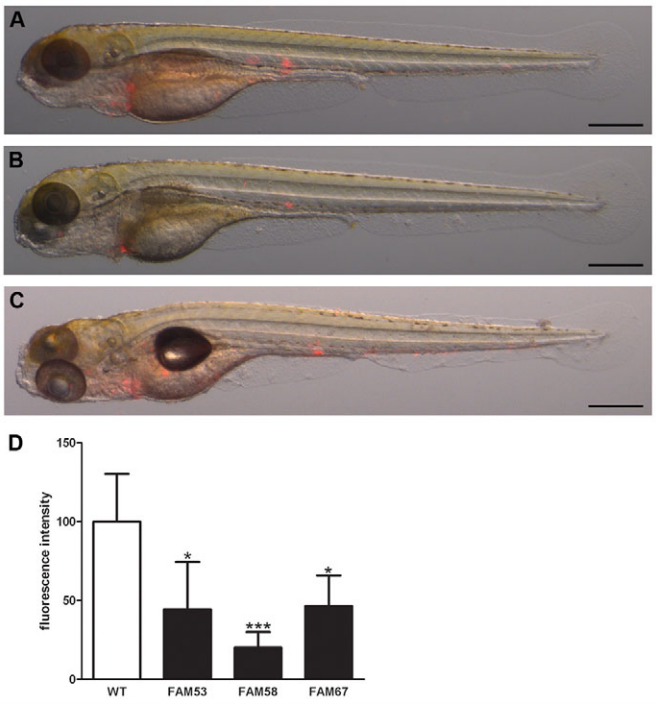

Fig. 2. Three out of 200 transposon mutants were identified as early granuloma mutants. Infection of embryos with mutants FAM53, FAM58 and FAM67 reproducibly resulted in either smaller or fewer early granulomas at 5 dpi, as compared with the wild type (see Fig. 1B). (A-C) Representative overlays of brightfield and fluorescent images of embryos infected with 71 CFUs of mutant FAM53 (A), 70 CFUs of mutant FAM58 (B) and 86 CFUs of mutant FAM67 (C) are shown. Scale bars: 500 μm. (D) Relative levels of infection determined by automated quantification of fluorescent pixels. The results represent mean + standard deviation of all experiments performed (n=3 to 9) (*P<0.029, ***P<0.001, unpaired Student's t-test).

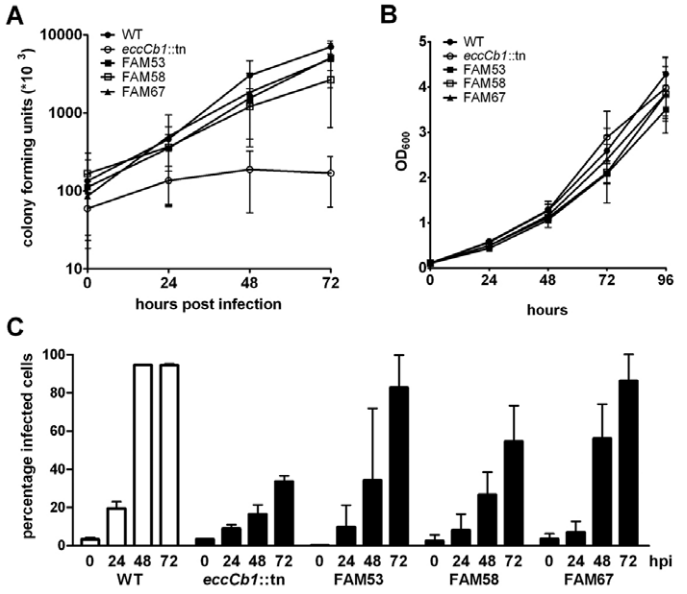

Fig. 3. Intracellular growth and spread of early granuloma mutants. (A) Intracellular growth of *M. marinum* in THP1 cells. THP1 macrophage-like cells were infected at MOI 1 with wild-type Mma11 (WT), the *eccCb1*::tn mutant and the three early granuloma mutants. The number of CFUs was determined by lysing infected THP1 cells and plating lysates at the indicated time points. Figure shows mean ± standard deviation for three independent experiments. (B) Growth rate of bacteria in 7H9 medium. Results represent mean ± standard deviation of two independent replicates. (C) Intercellular spread of *M. marinum* in THP1 cells. THP1 cells were infected at MOI 1 with wild-type Mma11 (WT), the *eccCb1*::tn mutant and the three early granuloma mutants. Percentage of infected cells was determined by microscopic enumeration of bacilli within THP1 cells. Mean + standard deviation of two independent replicates are shown.

Altogether, these results indicate that two of the three early granuloma mutants are not defective for intracellular growth and spread. This means that our screen is able to identify genes that are specifically required for the onset of granuloma formation in vivo and, consequently, that our screen has an added value as compared with a macrophage screen.

Identification of genes involved in the initial steps of granuloma formation

In order to identify the genes that were mutated in the three early granuloma mutants, the transposon insertion sites were determined by ligation-mediated PCR and sequence analysis.

The mariner transposon of mutant FAM53 is inserted in *fadE33*, which encodes a probable acyl-CoA dehydrogenase. This gene is highly conserved among actinobacteria and has a predicted function in lipid degradation. To analyze whether this mutation has any effect on the lipid and mycolic acid content of *M. marinum*, thin layer chromatography was performed using various systems according to previously described protocols (Besra, 1998). No differences between wild-type and mutant FAM53 were observed either in terms of mycolic acid profiles, extractable apolar lipid systems A-D, and polar lipid systems D and E (data not shown). These results indicate that the observed granuloma-deficient phenotype is probably not due to an alteration of cell wall lipids in the FAM53 mutant.

As mentioned previously, ESX-1 mutants are known to be delayed in granuloma formation (Gao et al., 2004; Volkman et al., 2004). Therefore, we expected to identify ESX-1 mutants in our in vivo granuloma screen. Mutant FAM58 indeed has a transposon insertion in the ESX-1 cluster, although the transposon is not inserted in one of the known ESX-1 genes. The exact insertion site of the mariner transposon is ten base pairs upstream of the gene *espL* (*mmar_5456*) and 27 base pairs downstream of *espB* (*mmar_5457*). Both expression and secretion of EspB were not impaired in mutant FAM58, as was determined by an immunoblot with an antibody directed against EspB of *M. tuberculosis* (Fig. 4A). Next, quantitative reverse-transcriptase (RT)-PCR was performed on Mma11 wild-type and mutant FAM58 to analyze transcription levels of *espL* and *espB* (Fig. 4B). As a control, the level of *eccCb1* transcripts was determined using primers surrounding the transposon insertion site of the *eccCb1*::tn mutant. As expected, similar *eccCb1* transcription levels were observed in *M. marinum* wild-type and mutant FAM58, whereas *eccCb1* transcripts were not detected in the *eccCb1*::tn mutant. In agreement with the immunoblot results, no drastic differences were observed between wild-type and mutant FAM58 *espB* transcripts. By contrast,

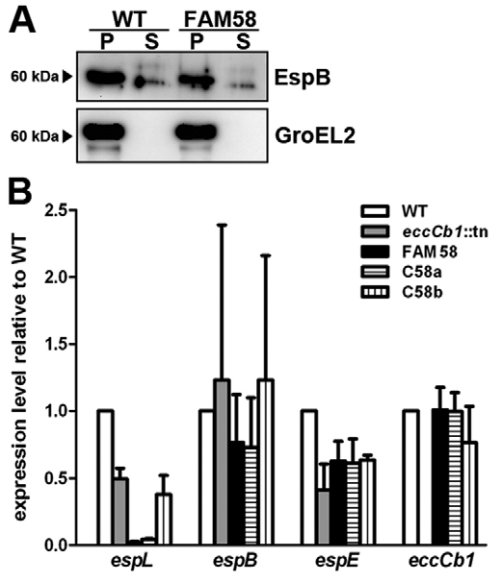

Fig. 4. Transcript levels of *espL* are strongly decreased in the FAM58 mutant. (A) Equivalent amounts of bacterial pellet (P) and culture supernatant (S) fractions of wild-type Mma11 and mutant FAM58 were separated on SDS-PAGE, immunoblotted and incubated with an antibody directed against EspB. As a fractionation control, the cytosolic protein GroEL2 was analyzed. (B) *espL* and *espB* transcription levels were analyzed for mutant FAM58, mutant FAM58 complemented with either *espL* (C58a) or the *espL-espB* operon (C58b) by quantitative RT-PCR and compared with wild-type Mma11 and the *eccCb1*::tn mutant. Additionally, transcript levels of *espE* and *eccCb1* were measured. Transcription levels were normalized to *sigA* because it has previously been shown that *sigA* mRNA levels remain unchanged during various growth conditions. Transcript levels of mutants and complemented mutants are presented as relative values compared with wild-type levels. Data shown are mean + standard deviation for three independent replicates.

transcription levels of *espL* were significantly reduced in mutant FAM58 (0.02 versus 1 – a 50-fold reduction). Therefore, we conclude that defective transcription of *espL* probably accounts for the early-granuloma-deficient phenotype.

Mutant FAM67 has a genetic link with the ESX-1 cluster as well. In this mutant, the transposon is also located in an intergenic region, the exact site being 19 base pairs downstream of gene *mmar_5425* and 364 base pairs downstream of *mmar_5426*. Interestingly, although *mmar_5425* is not located in the ESX-1 region itself, it shares homology with the ESX-1 gene *espK*. Furthermore, the transposon is inserted in a genomic region of 22 genes that is located immediately upstream of the ESX-1 locus and is specific for *M. marinum*. Out of these 22 genes, 20 are homologous to ESX-1 or ESX-1-associated genes (Stinear et al., 2008).

ESX-1 secretion of early granuloma mutants

The ESX-1 locus encodes a specialized secretion system responsible for the secretion of multiple proteins, including ESAT-6. ESAT-6 is an important mycobacterial virulence factor that is involved in phagosomal escape, cell lysis and cell-to-cell spread (Hsu et al., 2003; Gao et al., 2004; van der Wel et al., 2007; Smith et al., 2008). Furthermore, the reduction of expression and secretion of ESAT-6 is associated with delayed granuloma formation in both *M. tuberculosis* and *M. marinum* (Pym et al., 2002; Lewis et al., 2003; Volkman et al., 2004). Because mutant FAM58 was mutated in the ESX-1 region and also mutant FAM67 has a genetic link with ESX-1, for all three early granuloma mutants we analyzed expression and secretion of ESAT-6 and EspE, an ESX-1 secreted protein that is partially cell wall associated (Carlsson et al., 2009; Sani et al., 2010) (Fig. 5). In these experiments, we used GroEL2 as a marker for fractionation. As a negative control, the *M. marinum eccCb1*::tn mutant was used, which is known to be defective for ESX-1 secretion. As shown in Fig. 5A, ESAT-6 was detected in pellet fractions of wild-type Mma11 and all mutant bacteria, although in mutant FAM58 the protein was produced in slightly lower amounts. Interestingly, ESAT-6 secretion was strongly reduced in mutant FAM58, although secretion was not completely inhibited as it was for the *eccCb1*::tn mutant. This might be due to the fact that mutant FAM58 is not disrupted in one of the core components of the ESX-1 machinery, as is the case with mutant *eccCb1*::tn, but in an putative ESX-1 accessory gene, *espL*. It is known that ESAT-6 secretion is not only dependent on core components of the ESX-1 secretion system, but also on multiple ESX-1 substrates (Fortune et al., 2005; McLaughlin et al., 2007; Xu et al., 2007). We hypothesize that the residual ESAT-6 secretion of the FAM58 mutant contributes to the difference in infection level (20% versus 3.5%; compare Fig. 2D with Fig. 1E). Strikingly, although EspE was expressed intracellularly by the *eccCb1*::tn mutant, EspE could not be detected in any of the FAM58 fractions (Fig. 5B). In order to further investigate the nature of defective EspE expression in mutant FAM58, we analyzed *espE* transcription levels by quantitative RT-PCR. As shown in Fig. 4B, transcripts of *espE* in mutant FAM58 were moderately reduced as compared with those in wild type. However, transcription levels of *espE* in the *eccCb1*::tn mutant were even further decreased. These results demonstrate that EspL is not involved in the transcriptional regulation of *espE* and indicate that EspL might be required for the stability of this ESX-1 substrate.

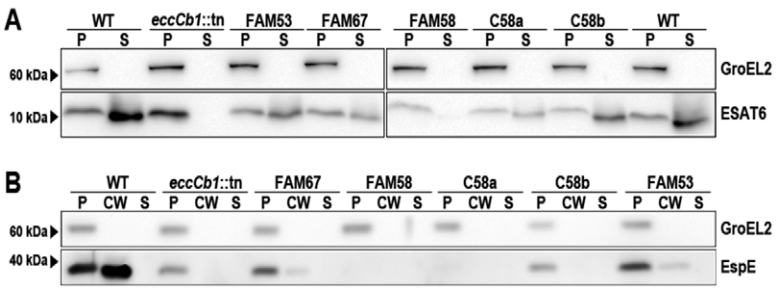

Fig. 5. ESX-1 secretion is affected in the FAM58 mutant. Equivalent amounts of bacterial cell pellet (P) and supernatant (S) fractions of the three early granuloma mutants and mutant FAM58 complemented with either *espL* (C58a) or the *espL-espB* operon (C58b) were analyzed for the presence of the ESX-1 substrates ESAT-6 (A) and EspE (B) by SDS-PAGE separation and immunoblot, and compared with those of wild-type Mma11 and the *eccCb1*::tn mutant. For immunoblots with anti-EspE antibodies, in addition to pellet and supernatant samples, extracted cell wall fractions (CW) were analyzed. As a fractionation control, the cytosolic protein GroEL2 was used.

Complementation of early-granuloma-deficient phenotype

To determine the genetic requirements for recovery of the early-granuloma-forming phenotype, mutant FAM58 was complemented with the intact version of *espL* or the *espL-espB* operon. Introduction of an integrative plasmid containing *espL* in mutant FAM58 (C58a) had only a slight effect on the mutant phenotype, i.e. onset of granuloma formation (Fig. 6C,E) and ESAT-6 secretion (Fig. 5A). These small changes might be explained by the fact that *espL* transcript levels are only marginally increased in this complemented mutant (see Fig. 4B; 0.04 versus 0.02 for mutant FAM58). For mutant FAM58 containing the entire *espL-espB* operon on an integrative plasmid (C58b), *espL* transcription levels were considerably increased, which probably resulted in increased initial granuloma formation (Fig. 6D,E) and ESAT-6 secretion (Fig. 5A), although none of these parameters reached wild-type levels. Surprisingly, although EspE expression was rescued in C58b, the protein was not detectable in the cell wall fraction (Fig. 5B). Our complementation experiments indicate that EspL is a newly identified ESX-1 component involved in ESAT-6 secretion and stable EspE expression.

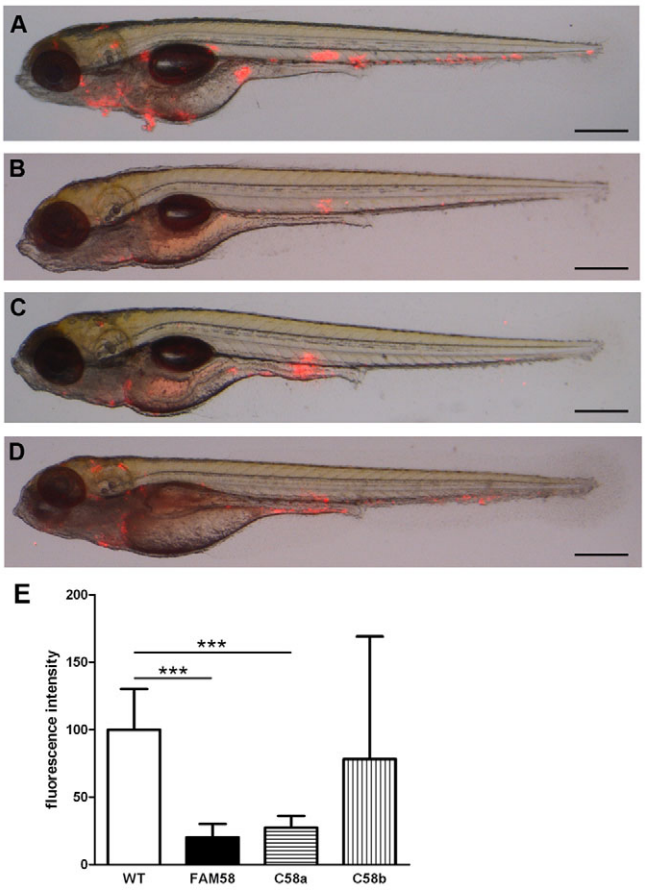

Fig. 6. Complementation of early granuloma mutant FAM58. Embryos 5 days after infection with wild-type Mma11, mutant FAM58 and FAM58 carrying a plasmid for expression of *espL* (C58a) or the *espL-espB* operon (C58b). (A-D) Representative images of embryos for all experiments performed (n=4 to 9) are shown. Infection doses were 137 CFUs for wild-type Mma11 (A), 128 CFUs for mutant FAM58 (B), 171 CFUs for C58a (C) and 127 CFUs for C58b (D). Scale bars: 500 μm. (E) Automated quantification of relative infection level. Results represent mean + standard deviation for all experiments performed (n=4 to 9) (***P<0.001, unpaired Student's t-test).

DISCUSSION

Granuloma formation is a hallmark of tuberculosis and over recent years it has become clear that mycobacteria actively promote the organization of these structures (Cosma et al., 2004; Volkman et al., 2004; Kahnert et al., 2007). However, thus far, bacterial factors that are involved in this process remain largely unknown. In this study, we have set up and demonstrated the use of a zebrafish embryo screen for the identification of bacterial genes involved in the initiation of mycobacterial granuloma formation. In order to find mycobacterial genes involved in the onset of granuloma formation, we analyzed 200 mutants from a random transposon mutant library of *M. marinum*. Although this number represents approximately merely 3% of the *M. marinum* genome, we identified three mutants that were reproducibly attenuated for early granuloma formation. None of these three mutants showed severely impaired replication in macrophages, and intercellular spread was only reduced in mutant FAM58. Apparently, granuloma formation goes beyond bacterial persistence in macrophages. This is not surprising, given that the development of a complex structure, such as a granuloma, depends on complicated processes involved in the recruitment and activation of immune cells. Moreover, the conditions experienced by mycobacteria inside granulomas are highly different as compared with those in macrophages (Chan et al., 2002). Therefore, we conclude that our in vivo approach for the identification of factors involved in the initiation of granuloma formation is an important tool to understand this complicated process.

One of the genes identified in this screen is *fadE33,* which is proposed to play a role in lipid metabolism. Mycobacteria have a unique cell envelope with an extraordinary high lipid content (Daffe and Draper, 1998). This outermost component of the bacteria contributes to their low permeability and resistance to many toxic compounds, and is involved in important host-pathogen interactions (Brennan and Nikaido, 1995; Karakousis et al., 2004). Furthermore, within granulomas mycobacteria adapt by switching from carbohydrate to fatty acid metabolism (Bishai, 2000). Thin-layer chromatography results did not demonstrate any dissimilarities in lipid contents of the cell wall between mutant FAM53 and wild-type bacteria. This indicates that attenuation of the FAM53 mutant is probably not due to an alteration of the cell envelope, so it might be that a metabolic defect is responsible for the reduced initiation of granuloma formation. This hypothesis is supported by the fact that *fadE33* is located in a genomic region with numerous genes that also have a predicted function in lipid catabolism.

The ESX-1 secretion system plays an important role in mycobacterial virulence and is studied extensively. Although the exact mechanism of attenuation is not known, it has been demonstrated that deletions of ESX-1 core components or substrates are associated with defects in phagosomal maturation arrest, membranolytic capacity, phagosomal escape, intracellular replication, intercellular spread and granuloma formation in mice and zebrafish (Hsu et al., 2003; Stanley et al., 2003; Gao et al., 2004; Guinn et al., 2004; Volkman et al., 2004; Tan et al., 2006; van der

Wel et al., 2007; Smith et al., 2008). So, it is not surprising that we have identified two mutants that have a link with ESX-1. Actually, the fact that ESX-1 mutations were picked up supports the reliability of our screen. It is, however, intriguing that the two ESX-1-associated genes that we found have not been associated with virulence before.

The gene that is mutated in FAM67, *mmar_5425*, is located in an *M. marinum* specific region encompassing 22 genes directly upstream of the ESX-1 region (Stinear et al., 2008). Except for one, all of these genes are homologous to ESX-1 genes. Strikingly, 13 of the 22 genes encode homologues of EspA, a protein that is secreted by the ESX-1 system. EspA is necessary for ESAT-6 and CFP-10 secretion and for virulence in mice (Fortune et al., 2005; Garces et al., 2010). The extended ESX-1 locus of *M. marinum* indicates that this organism has a large repertoire of putative ESX-1 substrates that might be involved in virulence and granuloma formation. *Mmar_5425* is highly similar to the N-terminal region of the ESX-1 gene *espK*. The exact role of EspK in virulence is not completely clear and deletion of its gene in *M. bovis* had no effect on virulence in a guinea pig infection model (Inwald et al., 2003). By contrast, an *M. marinum* mutant of *espK* was defective for ESAT-6 secretion and showed decreased cytolysis and cell spread in vitro (Gao et al., 2004). In contrast to the *espK* mutant, FAM67 did not have a defect in ESAT-6 secretion. Furthermore, FAM67 was not attenuated for either growth or spread in macrophages. Although the function of *mmar_5425* remains to be determined, we hypothesize that ESX-1 contributes to granuloma formation not only by ESAT-6 secretion, but also via additional mechanisms induced by other secreted proteins.

The second ESX-1-related gene that we identified, *mmar_5456* or *espL*, did have an effect on ESAT-6 secretion. We have demonstrated that *espL* is required for dissemination to macrophages, which is in line with a very recently published paper demonstrating that phagosomal maturation arrest in macrophages is affected in an *M. tuberculosis espL* mutant (Brodin et al., 2010). We expect that the lack of effective ESAT-6 secretion is responsible for the defective intercellular spread and, consequently, the limited onset of granuloma formation of the FAM58 mutant. Strikingly, the mutation in FAM58 also resulted in reduced expression or stability of EspE. Our results indicate that EspL is a new ESX-1 component important for expression and secretion of multiple ESX-1 substrates. These findings contribute to the complexity of ESX-1-dependent secretion, and emphasize the important role of ESX-1 in granuloma formation and virulence.

This study has demonstrated that our approach to screen for initial granuloma formation mutants with the zebrafish embryo *M. marinum* model results in the identification of interesting new virulence factors of mycobacteria. It is promising that screening of a relatively small amount of bacterial mutants identifies a number of exciting new virulence determinants. The ability to investigate our pathogen of interest in a natural host in an in vivo system contributes considerably to the strength of our approach. Our study adds to the understanding of currently known virulence determinants, such as ESX-1, but is also able to identify unknown virulence factors. These kinds of powerful in vivo screens will help to create new possibilities for the development of antibiotics, and mutants identified with such a screen might be potential new tuberculosis vaccines.

METHODS

Bacterial strains and growth conditions

Seven different *M. marinum* strains were used in this study. Two of them were fish isolates: strain E11 and E7 (Puttinaowarat et al., 1999). Strain 420472-4 was isolated from an infected snake and strain M, 9800607, 2000-01053 and 2001-00796 were originally isolated from human patients with fish tank granulomas (Ramakrishnan and Falkow, 1994; van der Sar et al., 2004). The *M. marinum* strains were grown at 30°C in Middlebrook 7H9 broth (Difco) with 10% Middlebrook albumin-dextrose-catalase (ADC; BD Bioscience) and 0.05% Tween-80 or on Middlebrook 7H10 agar (Difco) supplemented with 10% oleic-acid-albumin-dextrose-catalase (OADC; BD Bioscience). If *M. marinum* was cultured for electroporation, 2.5 mg/ml glycine was added once the cultures reached an optical density at 600 nm (OD_{600}) between 0.5 and 0.8 in order to increase electroporation efficiency. For secretion experiments, 7H9 medium supplemented with 0.04% ADC and 0.2% (w/v) dextrose was used. For cloning procedures, the *Escherichia coli* strain DH5α was used.

Plasmid transformation and transposon mutagenesis

The mycobacterial shuttle vector pSMT3-DsRed was constructed as a derivate of the pSMT3-eGFP vector (Hayward et al., 1999). The vector pSMT3-eGFP was digested with *Bam*HI and *Eco*RV to remove the gene encoding eGFP, which was replaced by a gene encoding DsRed that was excised as a *Bam*HI-*Pvu*II fragment from pGMDs3 (van der Sar et al., 2003). pSMT3-DsRed was electroporated into the Mma11 strain in order to be able to visualize bacteria. Transformants were selected on plates with 50 μg/ml hygromycin. Next, a transposon mutant library of Mma11 containing pSMT3-DsRed was generated with phage phiMycoMarT7, which contains the mariner-derived transposon Himar1 (Sassetti et al., 2001). It has been determined that transposition of the mariner transposon is random, and requires only the dinucleotide TA (Rubin et al., 1999). To select for transposon mutants, bacteria were grown on 7H10 plates supplemented with 50 μg/ml hygromycin and 25 μg/ml kanamycin.

Granuloma-activated promoter construct

The plasmid pSMT3-DsRed with the *gap7-eGFP* fusion was created by cloning a *Spe*I fragment that consists of the *gap7-eGFP* fusion and the kanamycin cassette of the *gap7* construct (Chan et al., 2002) into the *Xba*I site of the pSMT3-DsRed vector.

Mutant screen for initial granuloma formation in zebrafish embryos

Transposon mutant bacteria were grown until logarithmic phase, washed with 0.3% Tween-80 in phosphate buffered saline (PBS) to declump the bacteria, and resuspended in PBS containing 0.17% phenol red (Sigma) to aid visualization of the injection process. Wild-type *D. rerio* embryos at 28 hpf were dechorionated and infected by microinjection in the caudal vein. A total of 15 embryos were inoculated per mutant. To determine the exact number of bacteria injected into the embryos, the injection volume was also plated on 7H10 plates. Embryos were kept at 28°C in egg water (60 μg/ml instant ocean see salts) with 0.003% (w/v) 1-phenyl-2-thiourea (Sigma) to prevent melanization. At 5 dpi, bacterial infection was monitored with a Leica MZ16FA Fluorescence Stereo

Microscope. Brightfield and fluorescence images were generated with a Leica DC500 (DFC420C) camera, and early granuloma formation was analyzed visually and quantified with dedicated software (see below). During injection and microscopic examining, embryos were anesthetized in egg water with 0.02% (w/v) ethyl-3-aminobenzoate methanesulfonate salt (Sigma). All procedures involving zebrafish embryos were performed in compliance with local animal welfare laws.

Quantification of infection level

In order to quantify bacterial loads, fluorescent images of the infected zebrafish embryos were analyzed with specially designed, dedicated software (A.E.N., unpublished). For the analysis, three types of images were distinguished. First, fluorescent images of uninfected embryos were used. From these images, the average background intensity in each experimental run could be established. Second, as reference images, fluorescent images of embryos infected with wild-type bacteria were analyzed. Each reference image was thresholded by the background value obtained from the images of uninfected embryos. Per image, the sum of the pixels from the fluorescent red channel above background intensity was divided by the number of embryos. This was done for all images within a group and provides us a reference value of the amount of red fluorescent pixels per embryo at wild-type infection level. For each group of images of zebrafish embryos infected with mutant bacteria, the same calculation as for the reference images was realized and subsequently, the amount of fluorescent red pixels was provided as a percentage of the wild-type level.

Results are written to a comma separated file so that further statistical analysis and classification can be applied to the data. The measurement software was written in Delphi. The Graphical User Interface (GUI), written in English, allows for quick selection of experimental files and setup data files; it includes functions for folder processing and basic image manipulation. The actual processing is fully automated, which is very convenient in the medium-throughput context in which the experiments were realized. Different algorithms can be included in this processing environment so as to compare efficiency and precision of the algorithms (Nezhinsky and Verbeek, 2010) (for additional information, see http://bio-imaging.liacs.nl/galleries/granulomaload/).

Determination of bacterial loads of infected embryos

Pools of three embryos were dissociated in microcentrifuge tubes containing 100 µl 5% SDS in PBS. By incubation with 100 µl MycoPrep reagent (BD Bioscience; BBL 240862) for 10 minutes, under constant shaking, cells were lysed and decontaminated. To neutralize the solution, 1.8 ml of PBS was added and the homogenates were centrifuged for 15 minutes at 16,000 ***g***. 1.9 ml supernatant was removed and serial dilutions were plated on 7H10 plates.

THP1 infection assay

The human acute monocytic leukemia cell line THP1 was maintained on RPMI 1640 medium (Gibco) supplemented with 10% fetal calf serum (FCS), penicillin (100 units/ml) and streptomycin (100 µg/ml) at 37°C and 5% CO_2. Infection experiments with THP1 cells were carried out in 24-well plates. Cells were harvested by centrifugation for 10 minutes at 200 ***g*** and the pellet was resuspended in RPMI 1640 supplemented with FCS, penicillin and streptomycin to a density of approximately 3×10^5 cells/ml. In order to differentiate the THP1 cells into macrophage-like cells, 10 ng/ml phorbol myristate acetate was added and 1 ml of cell suspension was added to each well of a 24-well plate. For microscopy, THP1 cells were seeded on glass slides in 24-well plates. Plates were incubated overnight at 37°C and 5% CO_2. Medium was replaced by RPMI 1640 supplemented with FCS and plates were incubated overnight. For THP1 infection, bacteria were harvested by centrifugation for 10 minutes at 16,000 ***g***, washed with RPMI 1640 and suspended in RPMI 1640 with FCS. Bacteria were added to the cells at a multiplicity of infection of 1 and the cells were incubated for 2 hours at 30°C. Infected THP1 cells were washed three times with RPMI medium to remove extracellular bacteria and incubated in fresh RPMI with FCS for the indicated time points. To determine the amount of CFUs, cells were lysed by a 10-minute incubation with 1% Triton X-100 in PBS and bacteria were quantified by plating serial dilutions of lysates on 7H10 plates. For microscopic analysis, cells on glass slides were fixed with 4% paraformaldehyde for 24 hours, washed, mounted in VECTASHIELD (Vector Laboratories) and analyzed with a ZEISS Axioskop 40 microscope.

Identification of mutated genes

The transposon insertion sites of the early granuloma mutants were determined by ligation-mediated PCR as previously described (Abdallah et al., 2006). In addition to *Bam*HI-*Bgl*II digestion, chromosomal DNA was separately also digested with *Psp*OMI. For this restriction, the ligated linker consisted of the annealed oligonucleotides SalgD and PsPPT2 (for sequences see supplementary material Table S1). Furthermore, the mycomar T7-pr1 primer (supplementary material Table S1), located on the transposon, was also used in the PCR reaction.

SDS-PAGE and immunoblots

Mycobacterial cultures were grown to an OD_{600}~1. Pellet and supernatant fraction were separated by centrifugation. Bacterial cells were resuspended in PBS and subjected to bead-beating (Biospec) with glass beads (Sigma). Secreted proteins were precipitated from supernatant fractions with 10% (w/v) trichloroacetic acid (TCA). Samples were normalized to total protein concentration of the pellet fractions as determined by BCA Protein Assay (Pierce), mixed with SDS–polyacrylamide-gel-electrophoresis (SDS-PAGE) buffer, boiled for 10 minutes and separated by SDS-PAGE on 18% polyacrylamide gels for ESAT-6 and 12% gels for GroEL2. Proteins were visualized by immunoblotting with antibodies directed against ESAT-6 (Mab Hyb76-8) and GroEL2 (CS44; John Belisle, NIH, Bethesda, MD, contract No. AI-75320). The second antibody, GAMPO (American Qualex), was detected with enhanced chemiluminescence (ECL) using West Dura reagent (Pierce). For EspE analysis, prior to lysing pellet fractions, proteins were extracted from the cell wall by incubating pelleted bacterial cells with 0.5% Genapol X-080 in PBS for 30 minutes at room temperature. Extracted fractions were separated from bacterial cells by centrifugation and concentrated by TCA precipitation. Protein samples were prepared as described above and separated on 12% polyacrylamide gels. Proteins were visualized with anti-EspE antibodies (Genentech). The secondary

antibody, GARPO (Rockland), was detected with ECL. For immunoblots with anti-EspB antibodies, 500 ml bacterial cultures were grown to OD_{600}~0.7, after which bacterial pellets were washed with 7H9 medium supplemented with 0.2% (w/v) dextrose and resuspended in 500 ml of 7H9 with 0.2% (w/v) dextrose to grow overnight. Bacterial cells were harvested by centrifugation and pellet samples were prepared as described above. Supernatants were filtered through a 0.22 µm pore-size filter and concentrated with an ultra-filtration cell (Amicon; model 202) with a 3000 Da molecular mass cut-off membrane (Millipore). Concentrated supernatant protein samples were prepared as described above and samples were run on 10% gels. Proteins were detected with anti-EspB antibodies. The presence of the secondary antibody, peroxidase-labeled rabbit anti-rat-immunoglobulin, was visualized by ECL.

RNA isolation and quantitative RT-PCR

RNA was purified from bacterial cultures grown to an OD_{600}~1. Bacterial cells were disrupted by bead-beating in the presence of TRIzol Reagent (Invitrogen), and RNA was isolated according to the manufacturer's instructions. To eliminate genomic DNA contamination, RNA samples were treated with DNase I (Fermentas) and further purified with the RNeasy mini kit (Qiagen). cDNA was synthesized from 400 ng total RNA with the SuperScript VILO cDNA synthesis kit (Invitrogen), according to the protocol supplied by the manufacturer. Prior to use in subsequent PCR reactions, cDNA was diluted 1:10 and 1:100. Reactions were set up using EXPRESS SYBR GreenER qPCR SuperMix Universal (Invitrogen) and quantitative RT-PCR was performed with the LightCycler 480 Real-Time PCR System (Roche). Primers are listed in supplementary material Table S1. Data were normalized to the housekeeping gene *sigA*, which was used as an endogenous control (Manganelli et al., 2004).

Complementation of the mutants

The genes or gene regions in which transposons were inserted were PCR amplified with proofreading Pfu DNA Polymerase (Fermentas) using wild-type Mma11 genomic DNA as template. The oligonucleotides used to amplify *espL* and the *espL-espB* operon were esmm5456-F in combination with esmm5456-R or esmm5457-R (see supplementary material Table S1 for sequences). PCR products were cloned into the pJET1.2 cloning vector (Fermentas). To create an integrative vector, we used the pUC-INT-CAT vector (Abdallah et al., 2009). From this vector, we used a *Hin*dIII restriction fragment bearing the CAT cassette, the attP site and the integrase gene, and ligated this fragment into the *Hin*dIII site of the pJET vector that contained *espL* or the *espL-espB* operon. The resulting plasmid is an integrative, chloramphenicol-resistant vector. Plasmids were electroporated into the corresponding mutants and plated on 7H10 agar plates containing 50 µg/ml hygromycin and 30 µg/ml chloramphenicol. To confirm correct genome insertion, a PCR was performed with primers surrounding the integration site; wbINTgen and wbINTpls (see supplementary material Table S1), and with primers specific for the inserted genes.

ACKNOWLEDGEMENTS

We thank Fredericke Hannes, Eveline Weerdenburg and Corinne ten Hagen-Jongman for technical support, and Wim Schouten for his expert technical assistance. The *gap7* construct was a kind gift of Lalita Ramakrishnan (University of Washington, WA). We are grateful to Ida Rosenkrands (Statens Serum Institute, Denmark) and Florence Pojer (EPFL, Switzerland) for anti-ESAT-6 and anti-EspB antibodies. This research was supported by the Smart Mix Programme of the Netherlands Ministry of Economic Affairs and the Netherlands Ministry of Education, Culture and Science.

COMPETING INTERESTS

The authors declare that they do not have any competing or financial interests.

AUTHOR CONTRIBUTIONS

E.J.M.S., G.S.B., C.M.J.E.V.-G., W.B. and A.M.v.d.S. conceived and designed the experiments. E.J.M.S., T.S., S.K.R.H. and S.S.G. performed the experiments. A.E.N. and F.J.V. designed and implemented the software program. E.J.M.S., W.B. and A.M.v.d.S. wrote the paper.

TRANSLATIONAL IMPACT

Clinical issue

About 1.6 million people a year still die from tuberculosis (TB), and the disease is a major unresolved global health problem. The causative agent of TB is the bacterium *Mycobacterium tuberculosis*, which infects alveolar macrophages when it is inhaled as an aerosol. Macrophages are activated upon being infected, and recruit other macrophages, neutrophils and lymphocytes to cause the characteristic granulomas, or tubercles, that are the hallmark of TB. Granulomas are a double-edged sword: on the one hand they prevent the spread of *M. tuberculosis* throughout the body, but on the other hand they permit local multiplication of the bacteria and cause tissue destruction, thereby favouring transmission of the tubercle bacillus. In recent years, it has become clear that mycobacteria encode virulence factors that actively promote the formation of granulomas. These factors are of great interest both as targets for new anti-TB therapeutics, and also for developing new vaccine strains that are attenuated for granuloma formation.

Most studies that aim to identify tuberculosis virulence determinants are performed in vitro but, because formation of granulomas requires complicated host-pathogen interactions, this characteristic is best studied in vivo. The zebrafish (*Danio rerio*) is a useful model to study mycobacterial infections, because it is the natural host of *Mycobacterium marinum* – a close genetic relative of *M. tuberculosis* – which causes a tuberculosis-like disease characterized by necrotic caseating ('cheese-like') granulomas similar to those seen in infected humans.

Results

This study describes the development of a genetic screen for virulence factors involved in granuloma formation in zebrafish. A library of 200 single gene mutants of *M. marinum* bacteria, made by random insertion of the mariner transposable element into the *M. marinum* genome, is used to infect embryos. Mutants are scored for their effects on early granuloma formation by quantifying clusters of bacteria expressing DsRed.

Using this screen, three mutants are isolated as potential novel virulence factors, two of which are linked to the ESX-1 secretion system, a key player in the initiation of granuloma formation. One of the genes, *espL*, is located within the ESX-1 gene cluster, and its disruption has a strongly negative effect on secretion of the ESX-1 substrates ESAT-6 and EspE.

Implications and future directions

This work describes a novel medium-throughput in vivo screen to analyze the molecular mechanisms involved in early granuloma formation. As an experimental tool, the approach has many advantages. Screening of even a small sample of mutants can result in the identification of novel virulence factors and, because zebrafish embryos are easy to obtain and handle, infections can be performed within a short period of 6 days. Many transgenic zebrafish lines and tools are now available, so the system is also very versatile. The zebrafish is therefore likely to be a successful infection model to delineate the host-pathogen interactions that lead to mycobacterial granuloma formation, and hence to accelerate the development of new TB treatments.

SUPPLEMENTARY MATERIAL

Supplementary material for this article is available at
http://dmm.biologists.org/lookup/suppl/doi:10.1242/dmm.006676/-/DC1

REFERENCES

Abdallah, A. M., Verboom, T., Hannes, F., Safi, M., Strong, M., Eisenberg, D., Musters, R. J., Vandenbroucke-Grauls, C. M., Appelmelk, B. J., Luirink, J. et al. (2006). A specific secretion system mediates PPE41 transport in pathogenic mycobacteria. *Mol. Microbiol.* **62**, 667-679.

Abdallah, A. M., Verboom, T., Weerdenburg, E. M., Gey van Pittius, N. C., Mahasha, P. W., Jimenez, C., Parra, M., Cadieux, N., Brennan, M. J., Appelmelk, B. J. et al. (2009). PPE and PE_PGRS proteins of Mycobacterium marinum are transported via the type VII secretion system ESX-5. *Mol. Microbiol.* **73**, 329-340.

Adams, D. O. (1976). The granulomatous inflammatory response. A review. *Am. J. Pathol.* **84**, 164-192.

Besra, G. S. (1998). Preparation of cell-wall fractions from mycobacteria. In *Methods in Molecular Biology: Mycobacteria Protocols* (ed. T. Parish and N. G. Stoker), pp. 91-107. Totowa, NJ: Humana Press.

Bishai, W. (2000). Lipid lunch for persistent pathogen. *Nature* **406**, 683-685.

Brennan, P. J. and Nikaido, H. (1995). The envelope of mycobacteria. *Annu. Rev. Biochem.* **64**, 29-63.

Brodin, P., Poquet, Y., Levillain, F., Peguillet, I., Larrouy-Maumus, G., Gilleron, M., Ewann, F., Christophe, T., Fenistein, D., Jang, J. et al. (2010). High content phenotypic cell-based visual screen identifies Mycobacterium tuberculosis acyltrehalose-containing glycolipids involved in phagosome remodeling. *PLoS Pathog.* **6**, pii: e1001100.

Broussard, G. W. and Ennis, D. G. (2007). Mycobacterium marinum produces long-term chronic infections in medaka: a new animal model for studying human tuberculosis. *Comp. Biochem. Physiol.* **145C**, 45-54.

Carlsson, F., Joshi, S. A., Rangell, L. and Brown, E. J. (2009). Polar localization of virulence-related Esx-1 secretion in mycobacteria. *PLoS Pathog.* **5**, e1000285.

Chan, K., Knaak, T., Satkamp, L., Humbert, O., Falkow, S. and Ramakrishnan, L. (2002). Complex pattern of Mycobacterium marinum gene expression during long-term granulomatous infection. *Proc. Natl. Acad. Sci. USA* **99**, 3920-3925.

Cosma, C. L., Humbert, O. and Ramakrishnan, L. (2004). Superinfecting mycobacteria home to established tuberculous granulomas. *Nat. Immunol.* **5**, 828-835.

Daffe, M. and Draper, P. (1998). The envelope layers of mycobacteria with reference to their pathogenicity. *Adv. Microb. Physiol.* **39**, 131-203.

Davis, J. M. and Ramakrishnan, L. (2009). The role of the granuloma in expansion and dissemination of early tuberculous infection. *Cell* **136**, 37-49.

Davis, J. M., Clay, H., Lewis, J. L., Ghori, N., Herbomel, P. and Ramakrishnan, L. (2002). Real-time visualization of mycobacterium-macrophage interactions leading to initiation of granuloma formation in zebrafish embryos. *Immunity* **17**, 693-702.

Flynn, J. L. and Chan, J. (2005). What's good for the host is good for the bug. *Trends Microbiol.* **13**, 98-102.

Fortune, S. M., Jaeger, A., Sarracino, D. A., Chase, M. R., Sassetti, C. M., Sherman, D. R., Bloom, B. R. and Rubin, E. J. (2005). Mutually dependent secretion of proteins required for mycobacterial virulence. *Proc. Natl. Acad. Sci. USA* **102**, 10676-10681.

Gao, L. Y., Guo, S., McLaughlin, B., Morisaki, H., Engel, J. N. and Brown, E. J. (2004). A mycobacterial virulence gene cluster extending RD1 is required for cytolysis, bacterial spreading and ESAT-6 secretion. *Mol. Microbiol.* **53**, 1677-1693.

Garces, A., Atmakuri, K., Chase, M. R., Woodworth, J. S., Krastins, B., Rothchild, A. C., Ramsdell, T. L., Lopez, M. F., Behar, S. M., Sarracino, D. A. et al. (2010). EspA acts as a critical mediator of ESX1-dependent virulence in Mycobacterium tuberculosis by affecting bacterial cell wall integrity. *PLoS Pathog.* **6**, e1000957.

Guinn, K. M., Hickey, M. J., Mathur, S. K., Zakel, K. L., Grotzke, J. E., Lewinsohn, D. M., Smith, S. and Sherman, D. R. (2004). Individual RD1-region genes are required for export of ESAT-6/CFP-10 and for virulence of Mycobacterium tuberculosis. *Mol. Microbiol.* **51**, 359-370.

Hayward, C. M., O'Gaora, P., Young, D. B., Griffin, G. E., Thole, J., Hirst, T. R., Castello-Branco, L. R. and Lewis, D. J. (1999). Construction and murine immunogenicity of recombinant Bacille Calmette Guerin vaccines expressing the B subunit of Escherichia coli heat labile enterotoxin. *Vaccine* **17**, 1272-1281.

Hsu, T., Hingley-Wilson, S. M., Chen, B., Chen, M., Dai, A. Z., Morin, P. M., Marks, C. B., Padiyar, J., Goulding, C., Gingery, M. et al. (2003). The primary mechanism of attenuation of bacillus Calmette-Guerin is a loss of secreted lytic function required for invasion of lung interstitial tissue. *Proc. Natl. Acad. Sci. USA* **100**, 12420-12425.

Inwald, J., Jahans, K., Hewinson, R. G. and Gordon, S. V. (2003). Inactivation of the Mycobacterium bovis homologue of the polymorphic RD1 gene Rv3879c (Mb3909c) does not affect virulence. *Tuberculosis (Edinb.)* **83**, 387-393.

Kahnert, A., Hopken, U. E., Stein, M., Bandermann, S., Lipp, M. and Kaufmann, S. H. (2007). Mycobacterium tuberculosis triggers formation of lymphoid structure in murine lungs. *J. Infect. Dis.* **195**, 46-54.

Karakousis, P. C., Bishai, W. R. and Dorman, S. E. (2004). Mycobacterium tuberculosis cell envelope lipids and the host immune response. *Cell. Microbiol* **6**, 105-116.

Lewis, K. N., Liao, R., Guinn, K. M., Hickey, M. J., Smith, S., Behr, M. A. and Sherman, D. R. (2003). Deletion of RD1 from Mycobacterium tuberculosis mimics bacille Calmette-Guerin attenuation. *J. Infect. Dis.* **187**, 117-123.

Mahairas, G. G., Sabo, P. J., Hickey, M. J., Singh, D. C. and Stover, C. K. (1996). Molecular analysis of genetic differences between Mycobacterium bovis BCG and virulent M. bovis. *J. Bacteriol.* **178**, 1274-1282.

Manganelli, R., Provvedi, R., Rodrigue, S., Beaucher, J., Gaudreau, L. and Smith, I. (2004). Sigma factors and global gene regulation in Mycobacterium tuberculosis. *J. Bacteriol.* **186**, 895-902.

McLaughlin, B., Chon, J. S., MacGurn, J. A., Carlsson, F., Cheng, T. L., Cox, J. S. and Brown, E. J. (2007). A mycobacterium ESX-1-secreted virulence factor with unique requirements for export. *PLoS Pathog.* **3**, e105.

Nezhinsky, A. E. and Verbeek, F. J. (2010). Pattern recognition for high throughput zebrafish imaging using genetic algorithm optimization. In *Lecture Notes in BioInformatics* (eds T. M. H. Dijkstra, E. Tsivtsivadze, T. Heskes and E. Marchiori), pp. 301-312. Berlin-Heidelberg: Springer.

Prouty, M. G., Correa, N. E., Barker, L. P., Jagadeeswaran, P. and Klose, K. E. (2003). Zebrafish-Mycobacterium marinum model for mycobacterial pathogenesis. *FEMS Microbiol. Lett.* **225**, 177-182.

Puttinaowarat, S., Thompson, K., Lilley, J. and Adams, A. (1999). Characterization of Mycobacterium spp isolated from fish by pyrolysis mass spectrometry (PyMS) analysis. Inland *Aquat. Anim. Health Res. Institute Newslett.* **8**, 4-8.

Pym, A. S., Brodin, P., Brosch, R., Huerre, M. and Cole, S. T. (2002). Loss of RD1 contributed to the attenuation of the live tuberculosis vaccines Mycobacterium bovis BCG and Mycobacterium microti. *Mol. Microbiol.* **46**, 709-717.

Ramakrishnan, L. and Falkow, S. (1994). Mycobacterium marinum persists in cultured mammalian cells in a temperature-restricted fashion. *Infect. Immun.* **62**, 3222-3229.

Ramakrishnan, L., Valdivia, R. H., McKerrow, J. H. and Falkow, S. (1997). Mycobacterium marinum causes both long-term subclinical infection and acute disease in the leopard frog (Rana pipiens). *Infect. Immun.* **65**, 767-773.

Ramakrishnan, L., Federspiel, N. A. and Falkow, S. (2000). Granuloma-specific expression of Mycobacterium virulence proteins from the glycine-rich PE-PGRS family. *Science* **288**, 1436-1439.

Rubin, E. J., Akerley, B. J., Novik, V. N., Lampe, D. J., Husson, R. N. and Mekalanos, J. J. (1999). In vivo transposition of mariner-based elements in enteric bacteria and mycobacteria. *Proc. Natl. Acad. Sci. USA* **96**, 1645-1650.

Sani, M., Houben, E. N., Geurtsen, J., Pierson, J., de Punder, K., van Zon, M., Wever, B., Piersma, S. R., Jimenez, C. R., Daffe, M. et al. (2010). Direct visualization by cryo-EM of the mycobacterial capsular layer: a labile structure containing ESX-1-secreted proteins. *PLoS Pathog.* **6**, e1000794.

Sassetti, C. M., Boyd, D. H. and Rubin, E. J. (2001). Comprehensive identification of conditionally essential genes in mycobacteria. *Proc. Natl. Acad. Sci. USA* **98**, 12712-12717.

Saunders, B. M., Frank, A. A. and Orme, I. M. (1999). Granuloma formation is required to contain bacillus growth and delay mortality in mice chronically infected with Mycobacterium tuberculosis. *Immunology* **98**, 324-328.

Smith, J., Manoranjan, J., Pan, M., Bohsali, A., Xu, J., Liu, J., McDonald, K. L., Szyk, A., LaRonde-LeBlanc, N. and Gao, L. Y. (2008). Evidence for pore formation in host cell membranes by ESX-1-secreted ESAT-6 and its role in Mycobacterium marinum escape from the vacuole. *Infect. Immun.* **76**, 5478-5487.

Stanley, S. A., Raghavan, S., Hwang, W. W. and Cox, J. S. (2003). Acute infection and macrophage subversion by Mycobacterium tuberculosis require a specialized secretion system. *Proc. Natl. Acad. Sci. USA* **100**, 13001-13006.

Stinear, T. P., Seemann, T., Harrison, P. F., Jenkin, G. A., Davies, J. K., Johnson, P. D., Abdellah, Z., Arrowsmith, C., Chillingworth, T., Churcher, C. et al. (2008). Insights from the complete genome sequence of Mycobacterium marinum on the evolution of Mycobacterium tuberculosis. *Genome Res.* **18**, 729-741.

Swaim, L. E., Connolly, L. E., Volkman, H. E., Humbert, O., Born, D. E. and Ramakrishnan, L. (2006). Mycobacterium marinum infection of adult zebrafish causes caseating granulomatous tuberculosis and is moderated by adaptive immunity. *Infect. Immun.* **74**, 6108-6117.

Talaat, A. M., Reimschuessel, R., Wasserman, S. S. and Trucksis, M. (1998). Goldfish, Carassius auratus, a novel animal model for the study of Mycobacterium marinum pathogenesis. *Infect. Immun.* **66**, 2938-2942.

Tan, T., Lee, W. L., Alexander, D. C., Grinstein, S. and Liu, J. (2006). The ESAT-6/CFP-10 secretion system of Mycobacterium marinum modulates phagosome maturation. *Cell. Microbiol.* **8**, 1417-1429.

Trede, N. S., Langenau, D. M., Traver, D., Look, A. T. and Zon, L. I. (2004). The use of zebrafish to understand immunity. *Immunity* **20**, 367-379.

van der Sar, A. M., Musters, R. J., van Eeden, F. J., Appelmelk, B. J., Vandenbroucke-Grauls, C. M. and Bitter, W. (2003). Zebrafish embryos as a model host for the real time analysis of Salmonella typhimurium infections. *Cell. Microbiol.* **5**, 601-611.

van der Sar, A. M., Abdallah, A. M., Sparrius, M., Reinders, E., Vandenbroucke-Grauls, C. M. and Bitter, W. (2004). Mycobacterium marinum strains can be divided into two distinct types based on genetic diversity and virulence. *Infect. Immun.* **72**, 6306-6312.

van der Wel, N., Hava, D., Houben, D., Fluitsma, D., van Zon, M., Pierson, J., Brenner, M. and Peters, P. J. (2007). M. tuberculosis and M. leprae translocate from the phagolysosome to the cytosol in myeloid cells. *Cell* **129**, 1287-1298.

Volkman, H. E., Clay, H., Beery, D., Chang, J. C., Sherman, D. R. and Ramakrishnan, L. (2004). Tuberculous granuloma formation is enhanced by a Mycobacterium virulence determinant. *PLoS Biol.* **2**, e367.

Xu, J., Laine, O., Masciocchi, M., Manoranjan, J., Smith, J., Du, S. J., Edwards, N., Zhu, X., Fenselau, C. and Gao, L. Y. (2007). A unique Mycobacterium ESX-1 protein co-secretes with CFP-10/ESAT-6 and is necessary for inhibiting phagosome maturation. *Mol. Microbiol.* **66**, 787-800.

Table S1. Oligonucleotides used in this study

Name	Sequence
SalgD	TAGCTTATTCCTCAAGGCACGAGC
PsPPT2	GGCCGCTCGTGCC
T7-pr1	CCCGAAAAGTGCCACCTAAATTGTAAGCG
espL-F	AGATGGACCCCCAAGTCG
espL-R	GGACCAACTTCCTTCAGCAG
espB-F	AATCTTGAACAGGGCAGACG
espB-R	TCCTCGACCTCGCCATAA
espE-F	CATTTGGGGTCAGTTGCTTT
espE-R	TGAGCGATGTTCTGGTTCAA
eccCb1-F	CTGGCGGAAACATCGGTAT
eccCb1-R	CACCCGGTGGACTTTGTC
sigA-F	GAAAAACCACCTGCTGGAAG
sigA-R	CGCGTAGGTGGAGAACTTGT
esmm5456-F	ACGAAAATGACACCACAGCA
esmm5456-R	AGTAGCCGTCAGGACAGTCG
esmm5457-R	ATCCTGCGTCACAACTTGGT
wbINTgen	CTACCAAGCTGCGCTACACC
wbINTpls	TCGTTTGTCAGCATCGAAAG